

# Particle Formation and Ordering in Strongly Correlated Fermionic Systems: Solving a Model of Quantum Chromodynamics

P. Azaria<sup>1</sup>, R. M. Konik<sup>2</sup>, P. Lecheminant<sup>3</sup>, T. Pálmai<sup>4</sup>, G. Takács<sup>4,5</sup>, and A. M. Tsvelik<sup>2</sup>

<sup>1</sup> *Laboratoire de Physique Théorique de Matière Condensée,  
Université Pierre et Marie Curie, CNRS,  
4 Place Jussieu, 75005 Paris, France*

<sup>2</sup> *Condensed Matter Physics and Materials Science Division,  
Brookhaven National Laboratory, Upton, NY 11973-5000, USA*

<sup>3</sup> *Laboratoire de Physique Théorique et Modélisation,  
CNRS UMR 8089, Université de Cergy-Pontoise,  
Site de Saint-Martin, F-95300 Cergy-Pontoise Cedex, France,*

<sup>4</sup> *MTA-BME “Momentum Statistical Field Theory Research Group,  
H-1111 Budapest, Hungary, Budafoki út 8,*

<sup>5</sup> *Department of Theoretical Physics, Institute of Physics,  
Budapest University of Technology and Economics,  
H-1111, Budapest, Hungary, Budafoki út 8.*

(Dated: December 9, 2024)

## Abstract

In this paper we study a (1+1)-dimensional version of the famous Nambu-Jona-Lasinio model of quantum chromodynamics (QCD2) both at zero and finite baryon density. We use non-perturbative techniques (non-abelian bosonization and the truncated conformal spectrum approach (TCSA)). When the baryon chemical potential,  $\mu$ , is zero, we describe a formation of fermion three-quark (nucleons and  $\Delta$ -baryons) and boson (two-quark mesons, six-quark deuterons) bound states. We also study at  $\mu = 0$  a formation of a topologically nontrivial phase. When the chemical potential exceeds the critical value and a finite baryon density appears, the model has a rich phase diagram which includes phases with density wave and superfluid quasi-long-range (QLR) order as well as a phase of a baryon Tomonaga-Luttinger liquid (strange metal). The QLR order results in either a condensation of scalar mesons (the density wave) or six-quark bound states (deuterons).

PACS numbers: 12.38.-t,12.38.Aw,11.10Kk

## I. INTRODUCTION

The famous Nambu-Jona-Lasinio (NJL) model [1] of particle physics is frequently used as a simplified model of Quantum Chromodynamics (QCD) where the Yang-Mills force is replaced by a point-like four fermion current-current interaction. The replacement does not affect the low energy sector of the theory.

The (1+1)-dimensional version of the NJL model along with its prototype QCD2 has been a subject of intense interest (see, for instance Refs. [2, 3] for reviews and Ref. [4] for more recent work) since here one can obtain non-perturbative results solving the problem of many-body bound states and obtaining a reliable description of the excitation spectrum. However, few results are available for the formation of baryons in the (1+1)-D NJL model with a bare quark mass which breaks the  $U(1)$  chiral symmetry of the model. This problem has been mostly investigated in the past by variational approaches [5] and in the large- $N$  limit for the model with an  $SU(N)$  symmetry [6].

In this paper, we study the non-perturbative spectrum and the zero-temperature phase diagram of the massive (1+1)-D NJL model with two flavors ( $SU(3)_{\text{color}} \times SU(2)_{\text{isospin}} \times U(1)$  symmetry). Our approach is based on non-abelian bosonization, conformal field theory (CFT) techniques [7, 8], and non-perturbative numerical calculations based on the truncated conformal spectrum approach (TCSA) [9–11]. Although non-abelian bosonization was applied to QCD2 before [3, 12, 13], its combination with TCSA is new and this allows us to obtain a comprehensive description of the problem beyond the semiclassical and large color number approximations. The new results include bosonized expressions for the baryon operators, nonperturbative results for the excitation spectrum in the zero chemical potential regime, and the phase diagram (see Fig. IV.6).

At zero baryon density (zero chemical potential), the model has two gapped phases separated by an Ising quantum critical point corresponding to the spontaneous breaking of a  $Z_2$  symmetry. The order parameter is the  $\gamma_5$  quark mass. In the language of condensed matter physics this corresponds to a spontaneous dimerization of an insulator [22]. This breaking emerges when the t'Hooft term [14] has positive coupling and is sufficiently strong. In the disordered phase the low energy spectrum consists of isospin  $I = 1/2$  and  $I = 3/2$  baryons (three-quark bound states),  $I = 0, 1$  six-quark bound states (deuterons and dibaryons), and at least eight mesons (quark-antiquark bound states). The TCSA results for their masses

are given in Table IV.1.

When the chemical potential exceeds some critical value so that the density of baryons becomes finite, the phase diagram becomes more complicated. It includes several phases, each with a different quasi long range (QLR) order. Depending on the strength of the forward scattering and the hadron density, one may have a phase where the SU(2) isospin sector is gapped and hence the QLR does not originate from a Fermi surface instability, but emerges as a Bose condensation of the scalar mesons (a  $2k_F$  density wave (DW)) or the deuterons (superfluidity). The latter instability becomes dominant when the density exceeds some critical limit. In (1+1)-D there is no color superconductivity due to pairing of quarks contrary to what has been found in higher dimensions [15], but only the aforementioned superfluid phase of colorless six-quark bound states (the deuterons) as it was found in one-dimensional SU( $N$ ) cold fermions models [16]. There is also a critical phase (a baryon strange metal) of gapless baryons forming a Tomonaga-Luttinger liquid with gapped color degrees of freedom.

The main body of this paper is divided into four sections. In Section II we discuss the NJL model and the sigma model which emerges as its low energy equivalent. Here we also discuss the bosonized form of fermionic operators responsible for creation of mesons, baryons, and baryon bound states. In Section III we provide a simplified analysis of the excitation spectrum by means of a semiclassical approximation. In Section V, which contains most of our new results, we analyze the spectrum using TCSA. In Section IV we discuss the case of finite particle density. This section also contains a description of the model phase diagram.

## II. THE MODEL

The NJL model describes fermionic quarks with a bare mass  $m$  interacting via a current-current interaction. In (1+1)-dimensions, a Dirac spinor has two components corresponding to right- and left moving quarks. The Hamiltonian density of the left and right movers is

$$\mathcal{H} = i(-R_{j\sigma}^\dagger \partial_x R_{j\sigma} + L_{j\sigma}^\dagger \partial_x L_{j\sigma}) + m(L_{j\sigma}^\dagger R_{j\sigma} + \text{H.c.}) + gJ^A \bar{J}^A + g_f \mathcal{J} \bar{\mathcal{J}}, \quad (\text{II.1})$$

where  $R_{j\sigma}, L_{j\sigma}$  are annihilation operators of the right- and the left moving quarks,  $j = 1, 2, 3$  are color indices while  $\sigma = \uparrow, \downarrow$  are flavor indices corresponding to up and down quarks (we neglect all others in this treatment). The speed of light is set to one and a summation over

repeated indices is implied in the following.

We begin the treatment of this Hamiltonian through recourse to non-abelian bosonization (for additional details see Appendix A). To this end we identify the  $SU(3)_2$  Kac-Moody (KM) currents of right and left chirality:

$$J^A =: R_{j\sigma}^\dagger T_{jk}^A R_{k\sigma} :, \bar{J}^A =: L_{j\sigma}^\dagger T_{jk}^A L_{k\sigma} :,$$

where  $T_{jk}^A$  ( $A = 1, \dots, 8$ ) are the generators in the fundamental representation of the  $SU(3)$  group. In addition, there are also chiral  $U(1)$  currents:

$$\mathcal{J} =: R_{j\sigma}^\dagger R_{j\sigma} :, \bar{\mathcal{J}} =: L_{j\sigma}^\dagger L_{j\sigma} :.$$

The  $U(1)$  symmetry does not correspond to electric charge which we do not treat here. Instead the quarks carry baryonic charge. The interaction of the  $U(1)$  currents is an extra feature absent in (3+1)-dimensions. To analyze (II.1) using non-abelian bosonization, we use the fact that the Hamiltonian density of free Dirac fermions with symmetry  $U(1) \times SU(N) \times SU(M)$  can be represented as a sum of a Gaussian  $U(1)$  theory and two Wess-Zumino-Novikov-Witten (WZNW) CFT models of levels  $k = M$  and  $k = N$  respectively [17–19]. As a consequence, for each integer  $n$  one can write down  $n$ -point correlation functions of fermions in terms of products of  $n$ -point right and left conformal blocks of the  $U(1)$  Gaussian theory and the WZNW models.

At  $g > 0$  the model (II.1) is asymptotically free and acquires a mass gap  $M_q = \Lambda g^{2/3} \exp(-2\pi/3g)$  with  $\Lambda$  being the ultraviolet cut-off, in the color sector even if the bare mass  $m$  is zero. In the latter case the model is integrable [20]. We consider this dynamically generated quark mass,  $M_q$ , as the largest energy scale in the problem. The corresponding effective Lagrangian density for energies,  $E \ll M_q$ , is written in terms of the abelian and non-abelian Goldstone modes. It has a sigma model form [3, 12, 17]:

$$\mathcal{L} = \frac{K}{2} (\partial_\mu \theta)^2 + \text{WZNW}[SU(2)_3; G] + m^* \text{Tr}(e^{i\sqrt{2\pi/3}\theta} G + H.c.) + \lambda \cos(\sqrt{8\pi/3}\theta), \quad (\text{II.2})$$

where  $m^* \sim m$ ,  $G$  is an  $SU(2)$  matrix corresponding to the WZNW field (see Appendix A), and the term labeled WZNW stands for the WZNW Lagrangian on group  $SU(2)$  of level  $k = 3$ . In (II.2),  $\phi$  is a free massless bosonic field governing the  $U(1)$  density fluctuations and the Luttinger parameter  $K$  is related to the abelian coupling  $g_f$ , so that at  $|g_f| \ll 1$ ,  $K - 1 = O(g_f)$ . For attractive interactions,  $K < 1$ .

There is a direct analogy with (3+1)-D case as a similar sigma model [14] appears there as an effective low energy action for QCD and is used to study mesons and baryons with the latter appearing as solitons. The last term in Eqn. (II.2), absent in the original formulation (II.1), was introduced by t'Hooft [14] who argued that instantons generate the term proportional to the real part of the determinant of the U(2) matrix,  $\exp(i\sqrt{2\pi/3\theta})G$  (in condensed matter physics such a term is generated by Umklapp processes).

In Eqn. (II.2), the SU(2) matrix WZNW field  $G$  corresponds to the SU(2)<sub>3</sub> primary field  $\Phi^{(j)}$  with  $j = 1/2$  and has scaling dimension  $3/10$  [8]. Therefore the scaling dimension of the interaction term in Eqn. (II.2) with coupling constant  $m^*$  is

$$d_{m^*} = \frac{1}{6K} + \frac{3}{10},$$

so that it becomes irrelevant at  $K < 5/51$ . We note however that this interaction will generate at second order a relevant perturbation in the spin sector for  $K < 5/33$  so that in fact the theory is always gapped in the isospin sector – see section V. The instanton term,  $\cos(\sqrt{8\pi/3\theta})$ , in Eqn. (II.2) has scaling dimension  $d_\lambda = 2/(3K)$  and is relevant when  $K > 1/3$ . It becomes more relevant than the  $m^*$ -perturbation in Eqn. (II.2) when  $K > 5/3$ .

Below we list the most relevant operators local in terms of quarks which survive after the projection onto the SU(3) singlet sector given by the ground state of the SU(3)<sub>2</sub> WZNW model perturbed by its current-current interaction (see Appendix A). The operators with smallest scaling dimensions should correspond to mesons (U(1) neutral particles with Lorentz spin zero which are two-body bound states of quarks) and baryons (particles with Lorentz spin 1/2 and 3/2, formed as three-body bound states of quarks). After projection we obtain the following expressions for the meson operators at energy  $E \ll M_q$ :

$$\begin{aligned} \vec{M} &= R_{j\alpha}^\dagger \vec{\sigma}_{\alpha\beta} L_{j\beta} \sim e^{-i\sqrt{2\pi/3\theta}} \text{Tr}[\vec{\sigma}(G - G^\dagger)], \\ M^0 &= i(R_{j\alpha}^\dagger L_{j\alpha} - H.c.) \sim ie^{-i\sqrt{2\pi/3\theta}} \text{Tr} G + H.c., \end{aligned} \tag{II.3}$$

with  $\vec{\sigma}_{\alpha\beta}$  being the Pauli matrices. The right-moving baryon operators given by the three-quark SU(3) singlet bound states with respective Lorentz spins 3/2 and 1/2 are:

$$\Delta_{3/2}^{\alpha\beta\gamma} = \epsilon^{abc} R_{a\alpha} R_{b\beta} R_{c\gamma} \sim \exp(3i\sqrt{2\pi/3\varphi}) \mathcal{F}_{3/4}^{(3/2)}, \tag{II.4}$$

$$\begin{aligned} n_{1/2}^{\alpha\beta\gamma} &= \epsilon^{abc} R_{a\alpha} R_{b\beta} L_{c\gamma} \\ &\sim \exp[i\sqrt{2\pi/3}(2\varphi - \bar{\varphi})] \left[ \mathcal{F}_{2/5}^{(1)} \bar{\mathcal{F}}_{3/20}^{(1/2)} \right], \end{aligned} \tag{II.5}$$

where  $\varphi$  and  $\bar{\varphi}$  are the chiral components of the bosonic field,  $\theta = \varphi + \bar{\varphi}$ , and  $\mathcal{F}_{h_j}^{(j)}, \bar{\mathcal{F}}_{\bar{h}_{\bar{j}}}^{(\bar{j})}$  denote the  $SU(2)_3$  holomorphic and anti-holomorphic conformal blocks with isospin  $j, \bar{j} = 0, 1/2, 1, 3/2$  and weights  $h_j = \frac{j(j+1)}{5}$ . Their counterparts with opposite chirality are given by similar expressions with  $R$  replaced by  $L$ . As shown in Appendix A, the  $\Delta_{3/2}$  operator has isospin  $I = 3/2$  (respectively  $I = 1/2$ ) and is called a  $\Delta$ -baryon in the following, while the  $n_{1/2}$  operator has  $I = 1/2$  and is termed a nucleon.

There is also a bosonic (Lorentz spin 0) dibaryon operator with isospin  $I = 0$  and  $U(1)$  charge 2 (see Appendix A) which is the analogue of the deuteron. This operator is identified as follows in the low-energy  $E \ll M_q$  limit:

$$d_0 = (R_{1\alpha}\epsilon_{\alpha\beta}L_{1\beta})(R_{2\gamma}\epsilon_{\gamma\delta}L_{2\delta})(R_{3\eta}\epsilon_{\eta\rho}L_{3\rho}) \sim \exp(i\sqrt{6\pi}\phi)\text{Tr}(G + G^\dagger), \quad (\text{II.6})$$

where  $\phi = \varphi - \bar{\varphi}$  is the dual field to  $\theta$ . There is also a similar six-quark boson  $\vec{d}$  with isospin  $I = 1$  described by Eqn. (II.6) with  $(G + G^\dagger)$  replaced by  $i\sigma^a(G - G^\dagger)$ .

### III. SEMICLASSICAL ANALYSIS OF THE LOW-ENERGY SPECTRUM

To get a qualitative understanding of model (II.2) we can employ a semiclassical approximation which will be later augmented by the numerical analysis based on the TCSA. Despite its *a priori* restricted validity, our numerical results presented in the next section confirm that this analysis presents a qualitatively correct picture of the excitation spectrum.

To permit the semiclassical approximation, we represent the  $SU(2)$  matrix  $G$  as  $\hat{G} = \sigma\hat{I} + i\hat{\sigma}^a\pi_a$ ,  $\sigma^2 + \vec{\pi}^2 = 1$ . Using this, we can write the interaction term in in (II.2) as

$$V = m^* \cos(\sqrt{2\pi/3}\theta)\sigma + \lambda \cos(2\sqrt{2\pi/3}\theta). \quad (\text{III.1})$$

The ground state is determined by minima of  $V$  as the rest of the action (II.2) contains derivatives of the fields. The potential for  $\lambda = 0$  has degenerate minima at  $\sqrt{2\pi/3}\theta = 0, 2\pi n$ ,  $\sigma = -1$  and  $\sqrt{2\pi/3}\theta = \pi(1+2n)$ ,  $\sigma = 1$ . This fact suggests that there are two kinds of excitations: (i) fluctuations around the degenerate potential minima of (III.1) ( $\eta$  and  $\pi$  mesons); and (ii) kinks interpolating between these minima. The kinks interpolating between minima with the opposite sign of  $\sigma$  correspond to baryons, while the ones interpolating between the vacua with the same sign of  $\sigma$  are deuterons and isotriplet dibaryons. The small fluctuations constitute neutral isoscalar ( $\eta$ ) and isovector ( $\pi$ ) mesons. In Ref. [14] for

QCD3+1 it was predicted that there are eight mesons in total (one scalar and three vector mesons for each of the two vacua). In our numerics, we find these particles, but we also conclude that there are likely to be meson-meson bound states.

We have discovered that our numerical calculations indicate that we can make our semiclassical analysis quantitative. More precisely, the numerical calculations demonstrate that for  $0.3 < K < 1.5$  and  $\Lambda = 0$  the charge sector is well described by the sine-Gordon model. Hence for analytical calculations one can use the decoupling procedure where the bosonic exponent in Eq. (II.2) by its average and that similarly the U(1) charge sector can be well described by replacing  $\text{Tr}G$  by its vacuum average

$$m^* \text{Tr}(e^{i\sqrt{2\pi/3\theta}} G + \text{H.c.}) \rightarrow m^* (\langle e^{i\sqrt{2\pi/3\theta}} \rangle \text{Tr}G + e^{i\sqrt{2\pi/3\theta}} \langle \text{Tr}G \rangle + \text{H.c.}), \quad (\text{III.2})$$

where the theory that then describes the  $U(1)$  boson is sine-Gordon with coupling proportional to  $\langle \sigma \rangle$ . In this decoupling procedure, the scalar mesons correspond to the sine-Gordon breathers and the deuterons to the sine-Gordon solitons. As is known, the breathers disappear from the spectrum when the scaling dimension of  $\cos(\sqrt{2\pi/3\theta})$  becomes larger than 1 corresponding to  $K < 1/6$ . For  $K > 1/6$  there are bound states of the first breather corresponding to bound states of the scalar mesons. If we assume that this procedure continues to work for  $\lambda \neq 0$ , it will yield the double sine-Gordon model for the charge sector.

We can understand the effects of a nonzero  $\lambda > 0$  if we expand (III.1) around a particular minimum. For the sake of argument, we suppose  $m^* \sigma > 0$ :

$$V \sim A(\theta - \sqrt{3\pi/2})^2 + B(\theta - \sqrt{3\pi/2})^4, \quad (\text{III.3})$$

where  $B > 0$  and  $A$  may change sign depending on the mutual strength of  $m^*$  and  $\lambda$ . For  $A > 0$  the minimum is located at  $\theta = \sqrt{3\pi/2}$ . At  $A < 0$  the minima shift away from these points and  $A = 0$  corresponds to the Ising phase transition as in the double sine-Gordon model [21, 22, 25]. The transition occurs when  $\lambda^{1/(2-d_\lambda)} \sim m^{*1/(2-d_{m^*})}$ , that is at  $\lambda \sim (m^*)^{4(3K-1)/(51K/5-1)}$  and  $K > 1/3$ , i.e. when both operators in Eqn. (III.1) are relevant. When  $\lambda$  exceeds the critical value the minima of the potential (III.1) split so that the effective potential (Eqn. III.1) has two minima in the unit cell  $0 < \sqrt{2\pi/3\theta} < 2\pi$ . Then the bosonic vertex operator  $\sin(\sqrt{2\pi/3\theta})$  acquires a nontrivial vacuum expectation value. This implies that  $M_0$  (II.3) also has a non-trivial vacuum expectation value. This Ising order parameter having a finite expectation value might suggest that the condensate of mesons with zero

SU(2) isospin is topologically nontrivial in the sense of Kitaev [23]. However because this Ising order is occurring in an interacting system, we cannot conclude definitively that this phase is topological. In the condensed matter context a similar spontaneously dimerized phase emerges when one increases the electron-electron repulsive interaction in an insulator [22]. The splitting of the minimum of the effective potential creates a possibility that U(1) charged particles with isospin zero (deuterons) will have two different U(1) (baryon) charges corresponding to the short and long kinks of the field  $\theta$ .

When  $\lambda < 0$  we point to the possibility that two kinks (not kink-antikink) of the double sine-Gordon model may have bound states because an attractive potential in 1D generically leads to bound states. Such states would correspond to nuclei with baryonic charges higher than that of deuterium. However we will leave the resolution of this question to future work.

#### IV. NON-PERTURBATIVE NUMERICS

To go beyond the semiclassical approximation and to determine the coherence and stability of the low-energy excitations we have investigated the non-perturbative energy spectrum of model (Eqn. II.2) by TCSA. The bosonized form (II.2) permits a straightforward application of TCSA using its recent extension to treat deformations of conformal field theories of the WZNW-type [11].

In the case  $\lambda = 0$ ,  $m \neq 0$  and zero particle density we have found that the operators (II.3) and (II.6) indeed annihilate (create) coherent single-particle excitations. In particular  $d_0$  and  $\vec{d}$  destroy coherent excitons with isospin  $I = 0$  and  $I = 1$  respectively, with masses below the baryon continuum. Masses of the nucleons, mesons, and deuterons determined from the TCSA for different values of  $K$  are listed in Table IV.1. The mass ratios of the isoscalar particles turn out to be well described by the known exact result for the sine-Gordon model (see Eqn. IV.7), which is an important evidence for the validity of the approximation in Eqn. III.2). For the case where  $\lambda$  is nonzero, our numerics clearly indicate a phase transition at finite positive  $\lambda$ .

Below we discuss the application of TCSA to the model (II.2) and present a detailed analysis of the numerical results.

### A. The settings of the TCSA

Following standard procedures of TCSA (see e.g. [9–11, 25]), the quantum field theory is considered in a periodic spatial box of volume  $L$ . Introducing a unit of mass  $M$  as

$$m^* = M^{2-d_{m^*}} \quad d_{m^*} = \frac{1}{6K} + \frac{3}{10} \quad (\text{IV.1})$$

we can define a dimensionless volume parameter  $l = ML$  and measure energies in units of  $M$ . Mapping the coordinates  $(\tau, x)$  (where  $\tau$  is Euclidean time) to the complex plane

$$z = e^{\tau - ix} , \quad (\text{IV.2})$$

the dimensionless Hamiltonian can then be written as

$$h(l) = \frac{1}{M} H(L) = \frac{2\pi}{l} \left( L_0 + \bar{L}_0 - \frac{c}{12} \right) + \frac{l^{1-d_{m^*}}}{(2\pi)^{-d_{m^*}}} B_{m^*} + M^{d_\lambda - 2} \lambda \frac{l^{1-d_\lambda}}{(2\pi)^{-d_\lambda}} B_\lambda, \quad (\text{IV.3})$$

where  $L_0 + \bar{L}_0 - c/12$  is the conformal term and  $B_{m^*}$ ,  $B_\lambda$  are the matrices of the operators

$$\cos \left( \sqrt{2\pi/3} \theta(z, \bar{z}) \right) \left( \Phi_{-1/2, 1/2}^{(1/2)}(z, \bar{z}) - \Phi_{1/2, -1/2}^{(1/2)}(z, \bar{z}) \right) \quad (\text{IV.4})$$

particle species	$K = 0.4$	0.6	0.8	1.0	1.2	1.4
nucleon <sup>a</sup>	4.5	4.3	4.5	4.8	5.1	5.4
isoscalar meson	5.5	3.9	3.2	2.8	2.5	2.3
isovector meson	3.6	3.1	2.9	2.8	2.7	2.7
isoscalar deuteron	6.7	7.4	8.2	8.9	9.7	10.2
isovector deuteron	8.2	8.3	8.7	9.2	9.7	10.2

<sup>a</sup>The mass of the lightest baryon is estimated from the two-particle continuum in the baryonic charge two sector.

TABLE IV.1: Masses of the low-energy particles at  $\lambda = 0$  and zero particle density determined from TCSA in units  $M = (m^*)^{1/(2-d_{m^*})}$ . We estimate the error to be  $0.5M$  and  $1M$  in the meson and deuteron sectors, respectively, independent of  $K$ , and a relative accuracy to be one order of magnitude smaller.

and

$$\cos\left(2\sqrt{2\pi/3}\theta(z, \bar{z})\right), \quad (\text{IV.5})$$

respectively, at the point  $z = 1$  in the basis spanned by the conformal states. This space is truncated by keeping states for which

$$L_0 + \bar{L}_0 < N_{cut}, \quad (\text{IV.6})$$

for some cutoff value  $N_{cut}$ . With the cutoff in place, the resulting Hamiltonian can be numerically diagonalized. Due to translational invariance, the space can be split into sectors corresponding to the value of momentum; we restrict ourselves to discussing the zero-momentum sector, sufficient to obtain the information we need. In addition, it is possible to split the Hilbert space according to the value of baryonic charge and the third component of isospin, which makes the computation more efficient.

The matrix elements of the perturbing operators can be evaluated by reducing them to conformal field theory structure constants using conformal Ward identities (for example [24]) for an explicit description of the procedure which can be easily adapted to the Kac-Moody algebra considered here). Structure constants for diagonal primary fields in the SU(2) WZNW models have been obtained in [35], while those of the bosonic part are trivially obtained from free field theory. The inherent cut-off dependence is reduced using NRG techniques [10] to push  $N_{cut}$  to higher values, and analytic RG techniques to eliminate the cut-off dependence by introducing a running coupling following the procedure in [26–29]. We performed calculations in the parameter regime  $0.3 \leq K \leq 1.5$  with a step size of 0.1. Representative spectra are shown and analyzed below.

## B. Mesons

Initially we study the  $\lambda = 0$  case. We plot the zero momentum levels in the zero baryonic charge sector in Fig. IV.1 for the values  $K = 0.3, 1$  and  $1.5$ , with levels colored according to the isospin multiplet they belong to. The spectra are normalized by subtracting the ground state. There is another vacuum state which becomes exponentially degenerate with the lower ones for large volume, and accordingly all neutral particles come in two copies.

One-particle states can be identified by being below and separated from the dense continuum, and tending exponentially to a flat behavior. Some of these levels also show a dip

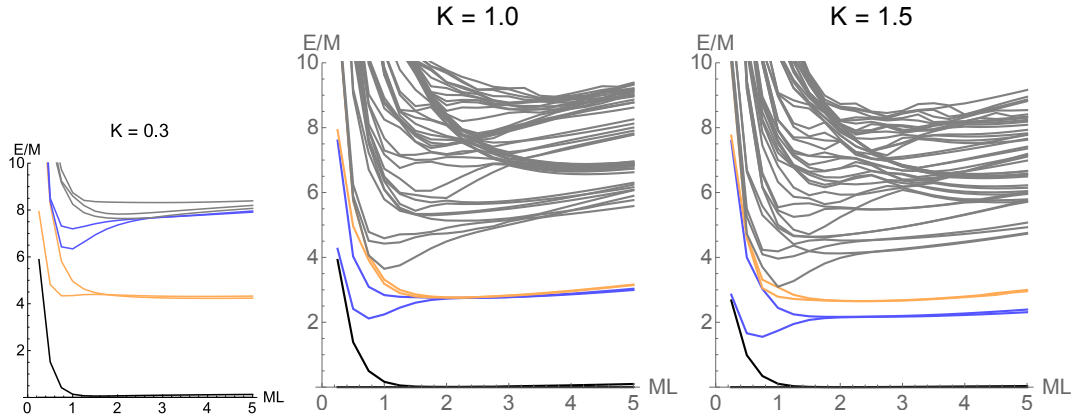


FIG. IV.1: Finite volume spectra in baryon charge zero sector at  $K = 0.3, 1.0, 1.5$ . The vacua (black), and the mesons (isosinglets – blue, isovectors – orange) are highlighted.

before becoming flat for larger volumes, which is a behavior that is typical for one-particle states due to so-called  $\mu$ -terms dominating their finite size corrections [30].

We find a meson isotriplet ( $\rho$ ) and an isosinglet ( $\omega$ ) meson, two copies for each. For  $K = 1$  the numerics shows them to be degenerate. When  $K > 1$  the triplet is heavier than the singlet, while for  $K < 1$  it is the mass of the singlet that is heavier than that of triplet.

From the ground state level we can also measure the bulk energy density, as shown in Fig. IV.2. For this we must perform a perturbative renormalization improvement to eliminate the leading dependence on the cutoff  $N_{cut}$ ; we follow the procedure used in [11]. This improvement leads to scaling the levels corresponding to different cut-offs on top of each other, and is more relevant for smaller  $K$ . The resulting vacuum energy densities  $B$  defined by the asymptotic behaviour

$$E_0(L) = -BL + \dots$$

where the omitted terms decay exponentially in the volume. The results of the linear fit are shown in the fourth subfigure of Fig. IV.2.

For excited states, we implemented further RG corrections corresponding to introducing a running coupling as in [26], however for this model the corrections induced by this proved to be negligible. We also added cut-off extrapolation improvements following [26]. Results from even and odd cut-offs can be extrapolated separately, and the extrapolated results are consistent, but they do not lead to any appreciable improvement of the results either.

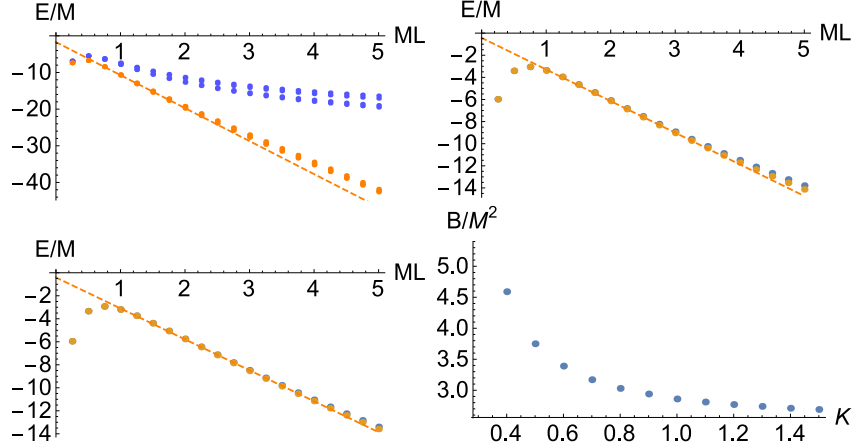


FIG. IV.2: Raw (blue) and renormalized (orange dots) vacuum energies for  $K = 0.3, 1.0, 1.5$  and at energy truncation  $E_{cut}/M = 8$ . The lines are linear fits yielding the energy densities in the bottom right panel.

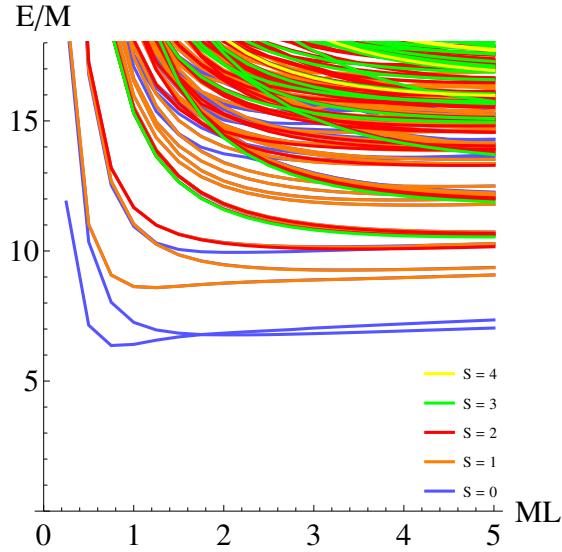


FIG. IV.3: Finite volume spectra for  $K = 0.3$  in the baryonic charge 2 sector, also showing the different isomultiplets formed by the various lines.

### C. Baryon bound states

Presently, the truncated conformal space approach can only access sectors of even baryonic charge. Sectors of odd baryonic charge correspond to half-integer isospin, i.e. transform under spinorial representations of the diagonal subgroup of the  $SU(2)_L \times SU(2)_R$  symmetry. Such states can only arise from fields that transform differently under the left and right

SU(2) groups. However, the structure constants of such fields are presently unknown; only the ones corresponding to diagonal fields are available [35]. In the sector with baryon charge 2 we find both isospin singlet and triplet bound states, as shown by the spectrum in Fig. IV.3. The isospin singlet state (coming in two copies due to the doubly degenerate vacuum is the analogue of the deuteron. However, the isotriplet has no analogue in 3+1 dimensional strong interactions; the reason is that in the isospin triplet channel the nucleon-nucleon potential is not attractive enough to form a bound state. However in one-dimensional space any attractive potential – no matter how shallow – leads to a bound state. From these considerations the appearance of the isotriplet bound state (two members of this multiplet would correspond to proton-proton and neutron-neutron bound states in the usual language of the strong interaction) is not so surprising. For higher values of  $K$  one of the triplets joins the continuum, i.e. the corresponding bound state disappears.

Assuming the validity of the semiclassical decoupling in Eqn. III.2 one expects the dynamics of isosinglet states will be dominated by the sine-Gordon like dynamics of the field  $\theta$  as the isospin degrees of freedom corresponding to the WZNW field  $G$  are frozen. The deuteron excitations correspond to sine-Gordon solitons, while the isosinglet mesons to the breathers. Their masses are known to be related by the exact relation

$$\frac{m_{\text{meson}}}{m_{\text{dibaryon}}} = 2 \sin \left( \frac{\pi/2}{12K - 1} \right), \quad (\text{IV.7})$$

which is comparable to the numerically observed mass ratio in Fig. IV.4 so providing numerical support for the decoupling approximation in Eqn. (III.2). Our plot also shows that this ratio does not hold in the isotriplet channel, which can be expected since these excitations have a more complicated structure due to the presence of the isospin degrees of freedom.

#### D. The case $\lambda \neq 0$

In Fig. IV.5 we show spectra at fixed  $K = 1.5$  and with increasing  $\lambda$ . The most prominent feature is a change in the vacuum structure: two additional vacua develop from the lines corresponding to the  $\lambda = 0$  singlet mesons. This supports the existence of the critical point established by our semiclassical analysis. For  $K = 1.5$  we estimate the critical value of the coupling to be  $M^{d\lambda-2}\lambda = 1.2$ . Above this value the vacua come in two pairs approaching

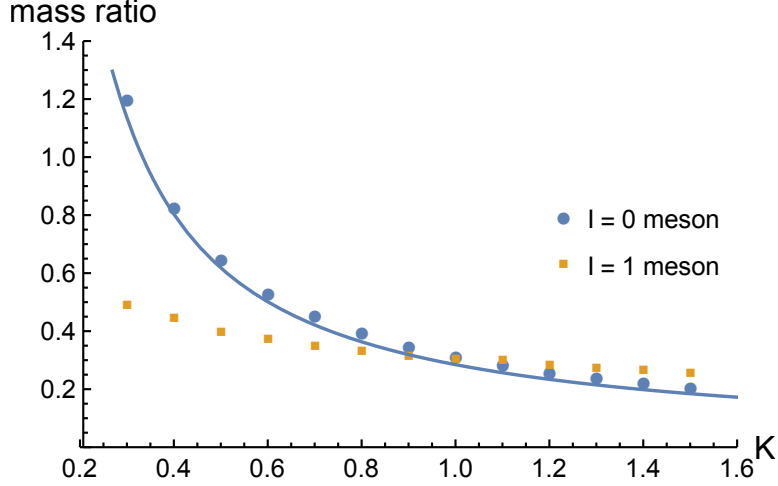


FIG. IV.4: Isoscalar and isovector meson/dibaryon mass ratios ( $m_{\text{meson}}/m_{\text{dibaryon}}$ ) and the approximate estimate for this in Eqn. IV.7.

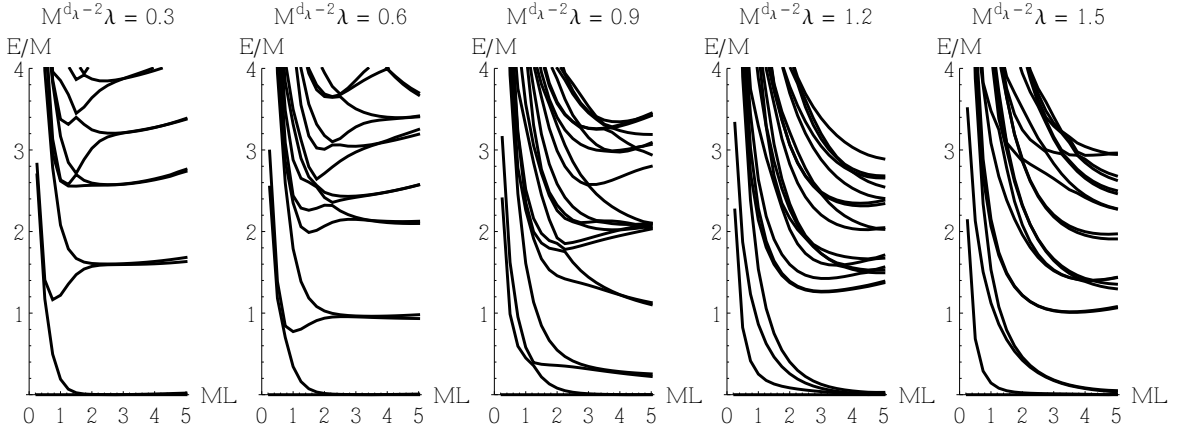


FIG. IV.5: Finite volume spectra at  $K = 1.5$  and different settings of the dimensionless coupling  $M^{d_\lambda-2}\lambda$  in baryonic charge zero sector.  $E_{\text{cut}}/M = 8$ .

each other algebraically. With increasing  $\lambda$  the triplet mesons join the continuum. We conclude therefore in the large  $\lambda$  phase that all eight mesons are unstable.

## V. FINITE BARYON DENSITY

New phases emerge when considering the model at finite baryon density by introducing into the Hamiltonian (II.1) a chemical potential,  $\mu$ , coupled to the baryonic charge (recall

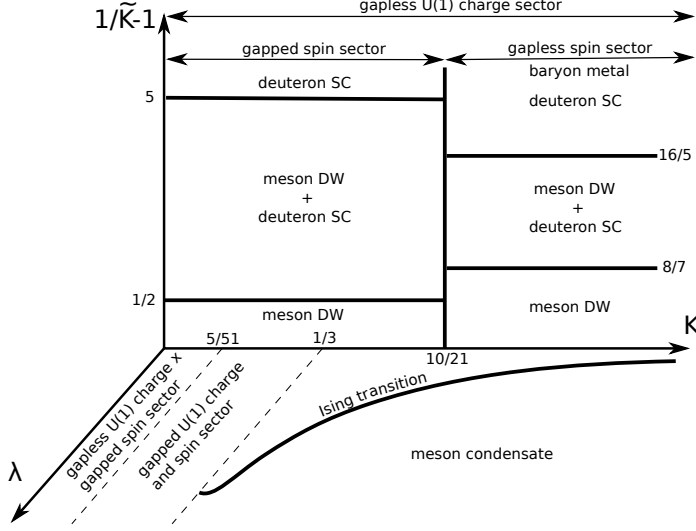


FIG. IV.6: The phase diagram of the NJL model as a function of the parameters  $K, \tilde{K}$  (Luttinger parameters at zero and finite chemical potential respectively) and  $\lambda$  (the coupling constant of the instanton term). Here  $\tilde{K}^{-1} - 1$  can be thought of as a proxy for the density of baryons in the Fermi sea. The  $\tilde{K} = 1, \lambda = 0$  axis is marked by three transitions. For  $K < 5/51$ , the theory is gapped in the (iso)-spin sector but gapless in the charge sector (treating the nominally irrelevant  $m^*$  perturbation at second order in perturbation theory). In contrast for  $5/51 < K$ , the relevant  $m^*$  perturbation leads to the theory being gapped in both of these sectors. For  $K > 1/3$  the instanton term becomes relevant. At finite  $\lambda > 0$  and  $K > 1/3$ , the  $K - \lambda$  plane is divided into two by an Ising-like transition. The ordered side of the transition is characterized by a meson condensate. The  $\tilde{K}^{-1} - K$  plane corresponds to the NJL model at finite baryon density induced by a chemical potential coupling to the U(1) charge. For  $K < 10/21$  the charge sector is gapless, but the spin sector is again gapped out by a perturbation generated at second order (note however that the value of  $K$  at which this happens differs from the zero baryon density phase). For  $K > 10/21$  we have a genuine baryon metal where both the spin and charge sectors are gapless. At finite baryon density the systems has different dominant quasi-long range orders, either deuteronic superconductivity (deuteron SC) or a meson density wave (meson DW). In certain regions of the finite density phase diagram, the instability to both of these orders is present (see text).

that the baryonic charge of quarks is  $1/3$ )

$$V_\mu = \mu(2/3\pi)^{1/2}\partial_x\theta. \quad (\text{V.1})$$

This explicit chemical potential term can be removed using the position dependent field redefinition  $\sqrt{2\pi/3}\theta \rightarrow \sqrt{2\pi/3}\theta + 2k_F x$ , where the Fermi vector is  $k_F \sim (\mu^2 - M_n)^{1/2}$ , with  $M_n$  being the nucleon mass. Since the chemical potential has no influence on the color sector, the ground state remains a color singlet and the quarks remain massive.

At finite baryon density the terms containing exponents of  $\theta$  field in the effective Lagrangian (II.2) become oscillatory. Normally such terms are dropped from the Lagrangian. However at second order in perturbation theory, the  $m^*$ -term coupling  $SU(2)_3$  with the  $U(1)$  boson may give rise to the term in the action

$$- A(\eta)(m^*)^2 \text{Tr} \Phi^{(1)}(x, \tau), \quad (\text{V.2})$$

where  $\Phi^1$  is the spin-1  $SU(2)_3$  primary field. At second order in perturbation theory in  $m^*$ , this field is generated by the operator product of the  $\text{Tr}G$  fields:

$$\begin{aligned} & e^{i(\sqrt{2\pi/3}\theta(x_1, \tau_1) + 2k_F x_1)} \text{Tr}G(x_1, \tau_1) e^{-i(\sqrt{2\pi/3}\theta(x_2, \tau_2) + 2k_F x_2)} \text{Tr}G(x_2, \tau_2) = \\ & e^{2ik_F(x_1 - x_2)} (x_{12}^2 + \tau_{12}^2)^{-d_{m^*} + d_{adj}/2} \text{Tr} \Phi^{(1)}(x_2, \tau_2) + \dots \end{aligned} \quad (\text{V.3})$$

Here  $d_{m^*} = 1/6K + 3/10$  and  $d_{adj} = 4/5$ . The operator (V.2) is generated if  $A(\eta)$ , the coefficient of the operator in the effective action given by,

$$A(\eta) = \int_{\Lambda_{eff}} d\tau dy \frac{\cos(2k_F y)}{(y^2 + \tau^2)^{(\eta+1)/2}}, \quad (\text{V.4})$$

converges at large distances where  $\eta = 2d_{m^*} - d_{adj} - 1$ . This integral comes equipped with an effective UV cutoff,  $\Lambda_{eff}$ , that reflects we have dropped all higher order terms in the OPE.  $\Lambda_{eff}$  is proportional to  $1/R$  where  $R$  is the size of the region where the integrand

$$\frac{\cos(2k_F y)}{(y^2 + \tau^2)^{(\eta+1)/2}},$$

in the above integral has significant support and encodes the fact that  $\text{Tr} \Phi^{(1)}(x)$  is really smeared over a region  $R$ . As  $K \rightarrow K_c$ ,  $R$  goes to  $\infty$  and  $A(\eta)$  vanishes. For  $K$  away from  $K_c$ , we can take  $\Lambda_{eff}$  to  $\infty$  and explicitly evaluate  $A(\eta)$ :

$$A(\eta) = \int_0^\infty dr J_0(2k_F r) r^{-2d_{m^*} + d_{adj} + 1} \sim k_F^{\eta-1} \frac{\Gamma(1/2 - \eta/2)}{\Gamma(1/2 + \eta/2)}, \quad (\text{V.5})$$

This integral is IR convergent if  $\eta = 1/3K - 6/5 > -1/2$  or  $K < K_c = 10/21$ . Note the effect that finite baryon density, i.e.  $k_F \neq 0$ , has. At zero density, the integral is instead IR convergent if  $\eta > 1$  which corresponds to  $K < 5/33$ .

Returning to finite density case, we furthermore can estimate  $R$  to be

$$R = \left( \sqrt{\frac{\pi}{2}} \frac{2^{-\eta} \Gamma(\frac{1-\eta}{2})}{\Gamma(\frac{1+\eta}{2})} \right)^{-\frac{1}{\eta+1/2}}. \quad (\text{V.6})$$

The effective action for  $K < K_c = 10/21$  is then

$$\mathcal{L} = \frac{\tilde{K}}{2} \left[ \frac{(\partial_\tau \theta)^2}{v_c} + v_c (\partial_x \theta)^2 \right] + \text{WZNW}[SU(2)_3; G] - \gamma \text{Tr} \Phi^{(1)}, \quad (\text{V.7})$$

Here  $\tilde{K}$  and the Fermi velocity,  $v_c$ , depend on the bare  $K$  and the chemical potential,  $\mu$ .  $\gamma$  is defined as

$$\gamma = A(\eta)(m^*)^2.$$

Because  $A(\eta)$  vanishes as  $K \rightarrow K_c$ , we see that the mass generated by the relevant perturbation,  $\text{Tr} \Phi^{(1)}$ , also goes to zero.

### A. Baryon metal phase, $K > K_c$

Hence we have two different situations depending on the strength of the attractive forward scattering in the original model. For sufficiently weak attractive interactions,  $K > K_c$ , the adjoint operator,  $\Phi^{(1)}$ , is not generated. Then at distances  $\gg k_F^{-1}$  the finite particle density phase is described by two critical models:

$$\mathcal{L} = \frac{\tilde{K}}{2} \left[ \frac{(\partial_\tau \theta)^2}{v_c} + v_c (\partial_x \theta)^2 \right] + \text{WZNW}[SU(2)_3; G], \quad (\text{V.8})$$

i.e. the U(1) Gaussian model and the  $SU(2)_3$  WZNW model describing the  $\pi$ -meson field. Their spectra are linear with velocities  $v_c$  and  $v_s$  respectively. Due to the vanishing gaps, this critical phase is a conductor that we call a baryon metal. The asymptotics of the correlation functions of the baryon operators can be extracted from the identification (II.4,II.5) and we find:

$$\begin{aligned} \langle \Delta_{3/2}(\tau, x) \Delta_{3/2}^\dagger(0, 0) \rangle &= \frac{Z_{3/2} \left( \frac{\tau_0^2}{\tau^2 + (x/v_c)^2} \right)^{\tilde{\eta}_{c,3/2}}}{[(\tau - ix/v_c)(\tau - ix/v_s)]^I}; \\ \langle n_{1/2}(\tau, x) n_{1/2}^\dagger(0, 0) \rangle &= \frac{Z_{1/2} \left( \frac{\tau_0^2}{\tau^2 + (x/v_c)^2} \right)^{\tilde{\eta}_{c,1/2}} \left( \frac{\tau_0^2}{\tau^2 + (x/v_s)^2} \right)^{\tilde{\eta}_{s,1/2}}}{[(\tau - ix/v_c)(\tau - ix/v_s)]^I}, \end{aligned} \quad (\text{V.9})$$

where  $\tau_0 \sim K_F^{-1}$  is an ultraviolet cutoff and  $\tilde{\eta}_{c,3/2} = \frac{3}{8}(\sqrt{\tilde{K}} - 1/\sqrt{\tilde{K}})^2$ ,  $\tilde{\eta}_{c,1/2} = \frac{1}{24}(1/\sqrt{\tilde{K}} - 3\sqrt{\tilde{K}})^2$ , and  $\tilde{\eta}_{s,1/2} = 3/10$ . The correlator of the left-moving particles is obtained by  $x \rightarrow -x$  and the one of the right- and the left- moving ones is zero.

From Eqn. (V.9) one can see that the baryons are incoherent: their single particle Green's functions have branch cuts which is the hallmark of a Tomonaga-Luttinger liquid [7]. In such a liquid there are no quasiparticles possessing both isospin and baryonic charges. Instead they decay into cascades of collective excitations ( $\pi$ -mesons) propagating with different velocities.

In this phase, there are instabilities to both deuteronic superconductivity and a meson density wave. The instability towards deuteronic superconductivity is revealed as a singularity in the response function of the deuteron operator (see Eqn. (II.6)). The scaling dimension of this field is  $d_{deut} = 3(\tilde{K}/2 + 1/10)$ , yielding a singular susceptibility as  $T \rightarrow 0$  for  $\tilde{K} \leq 7/15$ :

$$\chi_{deut} = \int_0^{1/T} d\tau \int dx \langle \hat{T} d_0(\tau, x) d_0^\dagger(0, 0) \rangle \sim T^{-2+2d_{deut}}, \quad (\text{V.10})$$

where  $T$  is temperature. We note that this instability can be in either the isospin  $I = 0$  or  $I = 1$  channels.

The meson density wave instability (with wavevector  $2k_F$ ) is, on the other hand, related to the scalar meson operator  $M_0 = R_{a\alpha}^\dagger L_{a\alpha} \sim e^{-i\sqrt{2\pi/3}\theta} \text{Tr}G$ . This scaling dimension of this order parameter is  $d_{DW} = \frac{1}{6\tilde{K}} + \frac{3}{10}$ . This order becomes singular at low temperatures for  $\tilde{K} \geq 5/21$ .

## B. Phase with gapped isospin excitations, $K < K_c$

At  $K < K_c$  the effective action (V.7) contains the relevant perturbation,  $\gamma \text{Tr}\Phi^{(1)}$ . Since the operator  $\Phi_{m,\bar{m}}^{(1)}$  acts only in the isospin sector the field  $\theta$  remains gapless with central charge  $c = 1$ . The  $SU(2)$  sector of (V.7) has been studied in [11, 31]. At  $\gamma > 0$  (the present case) it becomes massive and the spectrum consists of two degenerate massive triplets (pions). These baryons are incoherent, i.e. their correlation functions do not have poles in frequency-momentum plane, only branch cuts (see Appendix C).

Like for  $K > K_c$ , here there is an instability to deuteronic superconductivity. Unlike in the baryon metal phase at  $K < K_c$ , the amplitude of the  $SU(2)$  part of the deuteron operator,  $\text{Tr}(G + G^\dagger)$ , acquires a vacuum expectation value so that the operator can be replaced by  $d_0 \sim \exp(i\sqrt{6\pi}\phi)$ . The resulting scaling dimension is  $d_{deut} = 3\tilde{K}/2$ , yielding a singular susceptibility as  $T \rightarrow 0$  for  $\tilde{K} \leq 2/3$ .

The  $2k_F$  meson density wave can also be found here. Once the isospin sector is gapped  $\langle \text{Tr}G \rangle \neq 0$ , the scaling dimension of this order parameter is  $d_{DW} = 1/6\tilde{K}$ . Hence at  $1/6 < \tilde{K} < 2/3$  both the meson density wave and deuteronic superconductor susceptibilities are singular as  $T \rightarrow 0$ .

## VI. CONCLUSIONS

Our results demonstrate that 1+1D NJL model reproduces many properties expected for its 3+1D prototype [34]. We see, for example, that the masses of mesons and baryons are comparable to each other, as found in 3+1D. We stress that we have obtained these results for a realistic numbers of colors, i.e.  $N_c = 3$ . This was possible due to our use of the TCSA approach, a technique heretofore never applied to this particular problem. This powerful method enabled us to obtain masses of the multi-quark bound states including the six-quark deuteron, a notable achievement in the study of non-integrable strongly correlated systems. Although we have not explored this possibility, our theory can describe bound states of twelve quarks or more; they may emerge in the presence of the t'Hooft term with  $\lambda < 0$ . The spectrum that we have obtained numerical estimates for include stable fermionic solitons with quantum numbers of baryons: U(1) charge  $\pm 1$ , SU(2) isospin  $I = 1/2$  (nucleons) and  $I = 3/2$  ( $\Delta$ -baryons). There are also stable excitations with quantum numbers of mesons (U(1) neutral particles with isospin 0 and 1 and Lorentz spin 0), and six-quark bound states (isospin I =1 dibaryons and isospin I=0 deuterons).

A part of our work is related to the dense baryon matter. We have obtained the phase diagram which contains such phases as a baryon metal, analogous to non-Fermi liquid metallic states of one-dimensional condensed matter models, and various states with isospin gap and quasi-long range order, such as  $2k_F$  meson density wave as well as a superconducting phase of condensed deuterons.

### Acknowledgements

The authors are grateful to D. Gepner, L. Glazman, D. Kharzeev, G. Korchemsky, L. McLerran, G. Mussardo, R. Pisarski, and A. Zamolodchikov for discussions and interest in the work. AMT and RMK were supported by the U.S. Department of Energy (DOE),

Division of Materials Science, under Contract No. DE-AC02-98CH10886. TP was supported by a postdoctoral fellowship from the Hungarian Academy of Sciences (HAS), while TP and GT were also partially supported by the Momentum grant LP2012-50 of the HAS. PL would like to thank CNRS (France) for financial support (PICS grant).

### Appendix A: Non-abelian bosonization

The foundation of this method is the fact that the Hamiltonian density of free Dirac fermions with symmetry  $U(1) \times SU(N) \times SU(M)$  can be represented as a sum of a Gaussian theory and two Wess-Zumino-Novikov-Witten conformal field theories (WZNW CFT) models of levels  $k = M$  and  $k = N$  respectively [17–19]:

$$\begin{aligned} \sum_{j=1}^M \sum_{\sigma=1}^N i(-R_{j\sigma}^\dagger \partial_x R_{j\sigma} + L_{j\sigma}^\dagger \partial_x L_{j\sigma}) &= \text{WZNW}[SU(N)_M] + \text{WZNW}[SU(M)_N] \\ &+ \frac{1}{2} [(\partial_x \theta)^2 + (\partial_x \phi)^2]. \end{aligned} \quad (\text{A.1})$$

As a consequence, one can write down  $n$ -point correlation functions of fermions as a linear combination of products of  $n$ -point holomorphic and antiholomorphic conformal blocks of a  $U(1)$  Gaussian theory and the corresponding WZNW models. Hence, in the general case, such a decomposition must be understood not as an operator identity, as was the case for abelian bosonization, but only as an identity for the conformal blocks [3, 19]. Nevertheless, such identities will emerge at low energies in the theory given in Eqn. II.2 of the main text.

The Hamiltonian density of the  $SU(M)_N$  WZNW model is a sum of bilinears of its chiral Kac-Moody  $SU(M)_N$  currents  $J^A, \bar{J}^A$ :

$$\text{WZNW}[SU(M)_N] = \frac{2\pi}{N+M} [ : J^A J^A : + : \bar{J}^A \bar{J}^A : ], \quad (\text{A.2})$$

where  $: A :$  stands for the normal ordering of  $A$ . Each symmetry sector is decoupled. This remains true even when the interaction terms in Eqn. II.1 are added as they are given in terms of the currents of individual symmetry sectors. When  $M = 2$ , the  $SU(2)_N$  WZNW model Hamiltonian can be decomposed further and represented as a sum of a Gaussian  $U(1)$  model describing the Cartan subalgebra and a critical model of  $Z_N$  parafermions CFT [32]. We will need this decomposition in the discussion that follows.

It is reasonable to suggest that as soon as the interaction dynamically generates mass in the  $SU(3)$  sector that certain operators with zero Lorentz spin may acquire vacuum

expectation values. Here we will consider the dynamically generated quark mass  $M_q$  as very large. It then follows that all physical operators in the low-energy sector must be  $SU(3)$  singlets. The model of Eqn. II.2 represents a projection of the initial NJL Hamiltonian onto this color singlet space. To obtain operators acting in the low energy sector, we will need to project (II.3,II.4,II.5) onto the ground state  $|\text{GS}\rangle$  of the integrable model

$$\mathcal{H}_{\text{color}} = \text{WZNW}[SU(3)_2] + gJ^A\bar{J}^A = \frac{2\pi}{5}[:J^AJ^A: + : \bar{J}^A\bar{J}^A :] + gJ^A\bar{J}^A. \quad (\text{A.3})$$

We claim that after such reduction Eqns. (II.3,II.4,II.5) become operator identities. The proof is similar to the one given by Reshetikhin and Smirnov who performed the reduction of the sine-Gordon model to the minimal model with an integrable perturbation [33].

To perform the projection to the color singlet state we need to consider first the case when the bare quark mass and the instanton term are zero:  $m^* = 0, \lambda = 0$ . In this case, the sigma model in Eqn. (A.3) is gapless and critical and has an extended conformal symmetry. The underlying conformal field theory is

$$[U(1) \times SU(2)_3]_R \times [U(1) \times SU(2)_3]_L.$$

This symmetry is reduced to  $U(1) \times SU(2)$  as soon as  $m^* \neq 0$ .

Let us define the following fields in terms of  $\theta$  and its dual  $\phi$ :

$$\varphi = (\phi + \theta)/2, \quad \bar{\varphi} = (\theta - \phi)/2. \quad (\text{A.4})$$

At  $K = 1$  (this corresponds to  $g_f = 0$ ) these fields are chiral. For future purposes we need to know that the vertex operator

$$V_{n,m} = \exp[i\sqrt{2\pi/3}(n\varphi + m\bar{\varphi})] \quad (\text{A.5})$$

has conformal dimensions for general  $K$ :

$$\begin{aligned} h &= \frac{1}{48} \left[ (n+m)/\sqrt{K} + (n-m)\sqrt{K} \right]^2, \\ \bar{h} &= \frac{1}{48} \left[ (n+m)/\sqrt{K} - (n-m)\sqrt{K} \right]^2, \end{aligned} \quad (\text{A.6})$$

so that their conformal (Lorentz) spin is independent of  $K$ :

$$h - \bar{h} = (n^2 - m^2)/12. \quad (\text{A.7})$$

We will see that we will need exactly such vertex operators to construct the operators creating the mesons and the baryons.

Conformal blocks of the primary fields of the  $SU(N)_k$  WZNW model transform according to various representations of the  $SU(N)$  group. Their conformal dimensions are related to the quadratic Casimir operators of the corresponding representations [8]:

$$h_{rep} = \frac{C_{rep}}{k + N}. \quad (\text{A.8})$$

In particular, the conformal blocks of the  $SU(2)_3$  theory transforming according to the spin  $j$  representation will be denoted as

$$\mathcal{F}_h^{(j)}, \quad h_j = \frac{j(j+1)}{5}, \quad (\text{A.9})$$

with  $j = 0, 1/2, 1, 3/2$ . As far as the blocks for the  $SU(3)_2$  CFT are concerned, we will need only one of them, namely the one which transforms according to the representation with a single box Young tableau. The corresponding Casimir for the  $SU(N)$  is  $C_{rep} = (N - 1/N)/2$ , for  $N = 3$  it becomes  $4/3$  and the conformal dimension is  $4/15$ .

To illustrate the non-abelian bosonization procedure let us consider, for instance, the meson operators. They are bilinear in the fermionic operators, made from the right- and left- moving quarks. Hence they are bosonic operators with Lorentz spin 0. The symmetry considerations suggest that a meson operator must be a product of a bosonic exponent of field  $\theta$  and primary fields from the  $SU(2)$  and  $SU(3)$  groups respectively. Moreover, these fields have to transform according to the representations corresponding to the single box Young tableau:

$$R_{j\alpha}^+ L_{k\beta} = e^{-i\sqrt{2\pi/3\theta}} G_{\alpha\beta} D_{jk}, \quad (\text{A.10})$$

where  $G$  is the matrix of Eqn. (II.2) which transforms in the  $j = 1/2$  representation of the  $SU(2)$  isospin group and  $D$  is the  $SU(3)$  fundamental matrix field. According to (A.8) the conformal dimensions of these matrix fields for  $SU(N)_k$  model is given by the relation

$$h = \frac{N^2 - 1}{2N(k + N)},$$

so that for the  $G$  matrix it is  $3/20$  and the  $SU(3)$  matrix field  $D$  it is  $4/15$ . Then at  $K = 1$  (the noninteracting theory) the sum of all three dimensions is  $1/2$  as it must be. When the quarks becomes massive the operator from the  $SU(3)$  sector acquires a finite vacuum

average. Thus for the mesons we have

$$\vec{M} = \langle \text{GS} | R_{j\alpha}^+ \vec{\sigma}_{\alpha\beta} L_{j\beta} | \text{GS} \rangle \sim e^{-i\sqrt{2\pi/3}\theta} \text{Tr}[\vec{\sigma} G^+]. \quad (\text{A.11})$$

Now let us consider the operator for the right-moving nucleon. This operator is made of three quark fields. Since nucleon is a fermion, it has Lorentz spin 1/2 and therefore must contain two right- and one left-moving quarks. The bare conformal dimensions of such an operator is (1,1/2). The nucleon has isospin 1/2, hence the primary field in the SU(2) sector must transform as  $j = 1$  in the holomorphic and as  $j = 1/2$  in the antiholomorphic sector. The conformal dimensions of such operator are (2/5,3/20). In the SU(3) sector we have a color singlet. Here we suggest it is described by conformal blocks of the SU(3) matrix field  $D$  with conformal dimensions (4/15,4/15). The result is

$$\epsilon^{abc} R_{a\alpha} R_{b\beta} L_{c\gamma} = \exp[i\sqrt{2\pi/3}(2\varphi - \bar{\varphi})] \mathcal{F}_{2/5}^{(1)} \bar{\mathcal{F}}_{3/20}^{(1/2)} \text{Tr} D. \quad (\text{A.12})$$

It is easy to check that the conformal dimensions of the left hand side coincide with the ones of the right hand side. The projection on the color singlet state where  $\text{Tr} D$  condenses yields

$$n_{1/2}^{\alpha\beta\gamma} = \epsilon^{abc} \langle \text{GS} | R_{a\alpha} R_{b\beta} L_{c\gamma} | \text{GS} \rangle \sim \exp[i\sqrt{2\pi/3}(2\varphi - \bar{\varphi})] \mathcal{F}_{2/5,3/20}^{(1,1/2)}. \quad (\text{A.13})$$

We can repeat the same analysis for the  $\Delta$ -baryon operator with isospin  $I = 3/2$  of Eq. (II.4). Since the latter is made of three right-moving quarks in an SU(3) singlet state, we find:

$$\Delta_{3/2}^{\alpha\beta\gamma} = \epsilon^{abc} R_{a\alpha} R_{b\beta} R_{c\gamma} \sim \exp(i\sqrt{6\pi}\varphi) \mathcal{F}_{3/4}^{(3/2)} I_{SU(3)}, \quad (\text{A.14})$$

where  $I_{SU(3)}$  is the identity field of the SU(3)<sub>2</sub> CFT. By projecting out the color singlet state, the identification (II.4) is then reproduced.

At this point, it is interesting to express the baryonic operators in terms of  $Z_3$  parafermionic fields by exploiting the coset construction:  $SU(2)_3/U(1) \sim Z_3$  [32]. The SU(2)<sub>3</sub> primaries ( $\Phi_{m_j, \bar{m}_j}^{j, \bar{j}}$ ) are related to the  $Z_3$  parafermionic ones ( $f_{m, \bar{m}}^{l, \bar{l}}$ ,  $m = 2m_j, \bar{m} = 2\bar{m}_j, l = 2j, \bar{l} = 2\bar{j}$ ) by [32]:

$$\Phi_{m_j, \bar{m}_j}^{j, \bar{j}} = f_{m, \bar{m}}^{l, \bar{l}} : \exp \left( im \sqrt{\frac{2\pi}{3}} \varphi_s + i\bar{m} \sqrt{\frac{2\pi}{3}} \bar{\varphi}_s \right) :, \quad (\text{A.15})$$

where  $\varphi_s$  and  $\bar{\varphi}_s$  are the chiral components of a free bosonic field which accounts for the U(1) sector in the coset description. The  $Z_3$  primary fields are subject to the constraints:

$f_{m,\bar{m}}^{l,\bar{l}} = f_{m+3,\bar{m}+3}^{3-l,3-\bar{l}}$ ,  $f_{m,\bar{m}}^{l,\bar{l}} = f_{6+m,6+\bar{m}}^{l,\bar{l}}$ , where we take  $m$  to have periodicity 6, i.e.  $m+6 \equiv m$ . The  $\Delta$ -baryon operator (II.4) with isospin  $I = 3/2$  can then be expressed as a quartet field:

$$\Delta_{3/2,m} \sim \exp\left(i\sqrt{6\pi}\varphi\right) F_m, \quad (\text{A.16})$$

$$F_{m=\pm 3/2} = \exp\left(\pm i\sqrt{6\pi}\varphi_s\right), F_{m=\pm 1/2} = \exp\left(\pm i\sqrt{2\pi/3}\varphi_s\right) (\Psi, \Psi^+), \quad (\text{A.17})$$

where  $\Psi$  is the  $Z_3$  parafermionic current with holomorphic weight  $2/3$ . By introducing the isospin projection from

$$I^z = \sqrt{\frac{3}{2\pi}} \int dx \partial_x \Phi_s, \quad (\text{A.18})$$

$\Phi_s = \varphi_s + \bar{\varphi}_s$  being the total bosonic field, one can check that Eq. (A.17) has the correct isospin projection quantum numbers.

We now consider the right-moving nucleon field  $n_{1/2}$  (A.13) with isospin  $I = 1/2$  and Lorentz spin  $1/2$ . By using the identification (A.15), we find the following description for this doublet in the  $Z_3$  parafermionic basis:

$$n_{1/2,m=\pm 1/2} \sim \exp[i\sqrt{2\pi/3}(2\varphi - \bar{\varphi})] \exp[\pm i\sqrt{2\pi/3}(2\varphi_s + \bar{\varphi}_s)] (\mu, \mu^\dagger), \quad (\text{A.19})$$

where  $\mu$  is the  $Z_3$  disorder field with scaling dimension  $2/15$  [32]. Using the bosonized expression of the isospin projection (A.18), one can readily check that the operator (A.19) has the correct quantum numbers, i.e., isospin projection  $m = \pm 1/2$  and Lorentz spin  $1/2$ .

## Appendix B: Quantum numbers of baryons

We analyze in greater depth the excitations that interpolate between the different vacua of the semi-classical potential of Eq. (III.1) of the main text. There are two kinds of solitons. Type 1 solitons are those which interpolate between the vacua corresponding to different signs of  $\text{Tr}G$ . These particles carry both U(1) charge and isospin and so are baryons. The corresponding operators are given in Eqs. (II.4) and (A.16). Then there are type 2 solitons with isospin zero; they interpolate between the degenerate minima of the bosonic exponent  $(2\pi/3)^{1/2}\theta \rightarrow (2\pi/3)^{1/2}\theta + 2\pi n$ . The operator creating this particle is given by Eq. (II.6) of the main text. Type 2 solitons have baryon number 2.

We define the baryon U(1) charge as one. It is determined by the operator,

$$\hat{Q} = \sqrt{\frac{2}{3\pi}} \int dx \partial_x \theta. \quad (\text{B.1})$$

Let  $|q\rangle$  be an eigenfunction of  $\hat{Q}$  with eigenvalue  $q$ . Then using the identity

$$\hat{Q}e^{i2n\sqrt{2\pi/3}\varphi(x)}|q\rangle = (q + 2n/3)e^{i2n\sqrt{2\pi/3}\varphi(x)}|q\rangle, \quad (\text{B.2})$$

we establish that the above bosonic exponent of the chiral field  $\varphi$  raises the charge by  $2n/3$ . The baryon operator (II.4) has  $n = 3/2$  and hence creates a state of charge one. Therefore we conclude that this operator has a matrix element between the vacuum and a type 1 soliton state. Thus such solitons in our model are coherent particles.

Now we will show that the vacua  $\text{Tr}G = \pm 2$  really have structure. This becomes manifest in the  $Z_3$  parafermion representation. The mass term of Eqn. (II.2) of the main text in this representation reads as follows using the identification (A.15):

$$e^{i\sqrt{2\pi/3}(\theta+\Phi_s)}\sigma + H.c., \quad (\text{B.3})$$

where  $\sigma$  is the  $Z_3$  spin field with scaling dimension  $2/15$ .

Transitions between minima of this effective potential give rise to solitons. Stable (anti)solitons are charged ones with  $U(1)$  charge  $Q = \pm 1$ . They interpolate between the vacua as follows:

$$\begin{aligned} \sqrt{2\pi/3}\theta &\rightarrow \sqrt{2\pi/3}\theta \pm \pi, \\ \sigma^\dagger &\rightarrow e^{-2ki\pi/3}\sigma^\dagger, \quad \sigma \rightarrow e^{2ki\pi/3}\sigma, \\ \sqrt{2\pi/3}\Phi_s &\rightarrow \sqrt{2\pi/3}\Phi_s + \pi(\pm 1 - 2k/3), \quad k = 0, 1, 2. \end{aligned} \quad (\text{B.4})$$

Using the identity (A.18), these processes correspond to isospin projection  $I^z = \pm 3/2 - k$ . From Eq. (B.5), we observe that the transformation on the  $\sigma$  spin field corresponds to its  $Z_3$  charge assignment [32]. Operators  $F_{\pm 3/2}$  in Eq. (A.16) correspond to  $k = 0$  and hence to  $I^z = \pm 3/2$  as might be expected. The operator  $F_{1/2}$  in Eq. (A.17) has  $k = 1$  since the  $Z_3$  parafermion current  $\Psi$  carries a  $k = 1$   $Z_3$  charge [32] and therefore corresponds to  $I^z = 1/2$  as it should.

As we have already said, there are also charge neutral particles corresponding to

$$\begin{aligned} \sqrt{2\pi/3}\theta &\rightarrow \sqrt{2\pi/3}\theta \\ \sigma^\dagger &\rightarrow e^{-2ki\pi/3}\sigma^\dagger, \quad \sigma \rightarrow e^{2ki\pi/3}\sigma, \\ \sqrt{2\pi/3}\Phi_s &\rightarrow \sqrt{2\pi/3}\Phi_s + 2\pi(1 - k/3), \quad k = 0, 1, 2. \end{aligned} \quad (\text{B.5})$$

In principle they can decay into soliton-antisoliton pairs of charged ones. Without numerical calculations their stability cannot be assured. Such particles, if they exist, are likely to be  $I = 1$  mesons (pions). To look at dibaryons (charge 2) we can treat  $\text{Tr}G$  in Eq. (III.1) by a mean-field approximation, resulting in an effective double sine-Gordon model.

## Appendix C: Correlation functions

### 1. Zero density of baryons

In the zero density phase the charge and the isospin sector are coupled and the baryons exist as coherent particles. The coherent parts of their Green's functions are fixed by the Lorentz symmetry. For the nucleons we have the following time-ordered Euclidean Green's function:

$$\begin{aligned} \langle T n_{a1/2}(x, \tau) n_{b1/2}^\dagger(0) \rangle &= \theta(\tau) \int \frac{d\theta}{2\pi} e^{-m\tau \cosh(\theta) + imx \sinh(\theta)} e^{-\alpha_{1/2ab}\theta} \\ &\quad - \theta(-\tau) \int \frac{d\theta}{2\pi} e^{m\tau \cosh(\theta) - imx \sinh(\theta)} e^{-\alpha_{1/2ab}\theta}, \end{aligned} \quad (\text{C.1})$$

where the rapidity  $\theta$  parameterize the energy,  $m \cosh(\theta)$ , and momentum,  $m \sinh(\theta)$ , of a particle and  $a, b = R, L$  indicates whether the nucleon is right or left moving.  $e^{-\alpha_{1/2ab}\theta}$  is the matrix element squared between a nucleon state with rapidity,  $\theta$ , and the nucleon field operator. This matrix element is determined by Lorentz symmetry to be:

$$e^{\mp \frac{\theta}{2}} = \langle 0 | n_{R/L, 1/2}(0, 0) | 0 \rangle,$$

(up to a normalization constant). The factor of  $1/2$  in argument of the exponential reflects the nucleons having Lorentz spin  $1/2$  and so  $\alpha_{1/2ab} = \delta_{ab}$ . If we take the Fourier transform and then continue  $\omega \rightarrow -i\omega + \epsilon$ , we obtain

$$\langle n_{a1/2} n_{b1/2}^\dagger \rangle(\omega, q) = \frac{Z_{1/2}}{\omega^2 - \epsilon_{1/2}^2(q)} \begin{pmatrix} (q - \omega) & -\frac{M_{1/2}\omega}{\epsilon_{1/2}(q)} \\ -\frac{M_{1/2}\omega}{\epsilon_{1/2}(q)} & -(\omega + q) \end{pmatrix}_{ab}, \quad a, b = R, L, \quad (\text{C.2})$$

where  $Z_{1/2}$  is an overall normalization factor,  $M_{1/2}$  is the mass of the nucleon, and  $\epsilon_{1/2}(q) = \sqrt{M_{1/2}^2 + q^2}$ .

We can do the same for the  $\Delta$ -baryons. Here the relevant matrix element is

$$e^{\mp \frac{3\theta}{2}} = \langle 0 | \Delta_{R,L, 3/2}(0, 0) | 0 \rangle.$$

Fourier transforming as before we obtain

$$\langle \Delta_{a3/2} \Delta_{b3/2}^\dagger \rangle(\omega, q) = \frac{Z_{3/2}}{2M_{3/2}^2 \epsilon_{3/2}(q)} \times \left( \begin{array}{cc} \frac{(\epsilon_{3/2}(q)-q)^3}{\epsilon_{3/2}(q)-\omega} - \frac{(\epsilon_{3/2}(q)+q)^3}{\epsilon_{3/2}(q)+\omega} & \frac{-2M_{3/2}^3 \omega}{\omega^2 - \epsilon_{3/2}^2(q)} \\ \frac{-2M_{3/2}^3 \omega}{\omega^2 - \epsilon_{3/2}^2(q)} & \frac{(\epsilon_{3/2}(q)+q)^3}{\epsilon_{3/2}(q)-\omega} - \frac{(\epsilon_{3/2}(q)-q)^3}{\epsilon_{3/2}(q)+\omega} \end{array} \right)_{ab}, \quad a, b = R, L. \quad (\text{C.3})$$

We see that both the nucleon and  $\Delta$ -baryon Green's functions fall off as  $1/\omega$ .

## 2. Finite density of baryons

In the gapped phase of the dense baryon matter the spin excitations are gapped and the charge ones are not. The gapped excitations which determine the single baryon Green's functions are charge neutral solitons interpolating between different minima of the potential  $\text{Tr}G = \pm 2$ . The corresponding matrix elements (in the  $SU(2)_3$  sector of the theory) between these excitations are the baryon fields are again fixed by the Lorentz invariance:

$$\begin{aligned} \langle \theta | \mathcal{F}_{3/4}^{(3/2)}(\tau, x) | 0 \rangle &\sim e^{-3\theta/4} e^{-M_{3/2}(\tau \cosh \theta + i(x/v_s) \sinh \theta)} \\ \langle \theta | \mathcal{F}_{2/5}^{(1)} \mathcal{F}_{3/20}^{(1/2)}(\tau, x) | 0 \rangle &\sim e^{-\theta/4} e^{-M_{1/2}(\tau \cosh \theta + i(x/v_s) \sinh \theta)}. \end{aligned} \quad (\text{C.4})$$

Here we will consider only the part of the single baryon Green's function which originates from emission of this single massive soliton.

Generally for nucleons and the  $\Delta$ -baryons the Green's functions become (we focus only on the right-mover fields here)

$$\begin{aligned} \langle n_{R,1/2}(x, \tau) n_{R,1/2}^\dagger(0, 0) \rangle &= \frac{(\tau + \frac{i\mathbf{x}}{v_s})^{1/4}}{(\tau - \frac{i\mathbf{x}}{v_c})^{1/2} (\tau - \frac{i\mathbf{x}}{v_s})^{1/4}} \left( \frac{\tau_0^2}{\tau^2 + (\frac{\mathbf{x}}{v_c})^2} \right)^{\eta_{c,1/2}} K_{1/2}(M_{1/2}\rho) + \dots, \\ \langle \Delta_{R,3/2}(x, \tau) \Delta_{R,3/2}^\dagger(0, 0) \rangle &= \frac{(\tau + \frac{i\mathbf{x}}{v_s})^{3/4}}{(\tau - \frac{i\mathbf{x}}{v_c})^{3/2} (\tau - \frac{i\mathbf{x}}{v_s})^{3/4}} \left( \frac{\tau_0^2}{\tau^2 + (\frac{\mathbf{x}}{v_c})^2} \right)^{\eta_{c,3/2}} K_{3/2}(M_{3/2}\rho) + \dots, \\ \rho^2 &= \tau^2 + \left( \frac{\mathbf{x}}{v_s} \right)^2, \end{aligned} \quad (\text{C.5})$$

where  $\tau_0 \sim (k_F v_c)^{-1}$  is the ultraviolet cut-off, the dots stand for contributions which include more than one massive particle (for instance, one soliton and mesons).

We have been unable to perform the Fourier transform in full generality (i.e.  $v_c \neq v_s$  and  $\eta_{1/2,3/2} \neq 0$ ) and so we focus on the easiest case,  $v_c = v_s = v, \eta_{1/2,3/2} = 0$ . We note that while it is possible to consider the case of equal spin and charge velocities when  $\eta_{1/2,3/2} \neq 0$ , this gives rise to unphysical behaviour in the response functions at large  $\omega$ . Considering then this simplest case (which would hold for very low densities of baryons such that the velocities have not been renormalized) we find (with  $v_c = v_s = 1$ ):

$$\begin{aligned}
I_{1/2}(\omega, k) &\equiv \int d\tau dx e^{i\omega\tau - ikx} \langle n_{R,1/2}(x, \tau) n_{R,1/2}^\dagger(0, 0) \rangle; \\
I_{3/2}(\omega, k) &\equiv \int d\tau dx e^{i\omega\tau - ikx} \langle \Delta_{R,3/2}(x, \tau) \Delta_{R,3/2}^\dagger(0, 0) \rangle; \\
I_a(\omega, k) &= -4\pi \left( \frac{k - i\omega}{k + i\omega} \right)^a \frac{(\omega^2 + k^2)^a \Gamma(a + 1)}{2^a M_a^{2+a} \Gamma(1 + 2a)} {}_2F_1(a + 1, 1, 1 + 2a, -\frac{\omega^2 + k^2}{M_a}), \quad (\text{C.6})
\end{aligned}$$

where  $a = 1/2, 3/2$  for the nucleons/ $\Delta$ -baryons respectively.

Continuing  $\omega$  so as to obtain the retarded response, we plot the spectral weight (the imaginary part of  $I_a(-i\omega + \epsilon)$ ) for each of the nucleon and  $\Delta$ -baryon in Fig. (C.1). We see that this weight appears as a broadened  $\delta$ -function. In the zero baryon density phase, the spectral weight of the baryon propagators are only seen at  $\omega = k$ . But in the presence of finite baryon density, the baryons are no longer coherent particles and this weight is smeared over a finite energy range. We also the spectra function of the nucleons is much more peaked than that of the  $\Delta$ -baryons, indicating the nucleons remain considerably more coherent than their spin-3/2 counterparts in the presence of finite baryon density.

- 
- [1] Y. Nambu and G. Jona-Lasinio, Phys. Rev. **122**, 345 (1961).
  - [2] Y. Frishman and J. Sonnenschein, Phys. Rep. **223**, 309 (1993).
  - [3] Y. Frishman and J. Sonnenschein, *Non-Perturbative Field Theory* (Cambridge University Press, Cambridge, England, 2010).
  - [4] E. Katz, T. M. Tavares, and Y. Xu, arXiv:1405. 6727.
  - [5] L. L. Salcedo, S. Levit, and J. W. Negele, Nucl. Phys. B **361**, 585 (1991).
  - [6] C. Boehmer, U. Fritsch, S. Kraus, and M. Thies, Phys. Rev. D **78**, 065043 (2008); C. Boehmer, F. Karbstein, and M. Thies, Phys. Rev. D **77**, 125031 (2008).

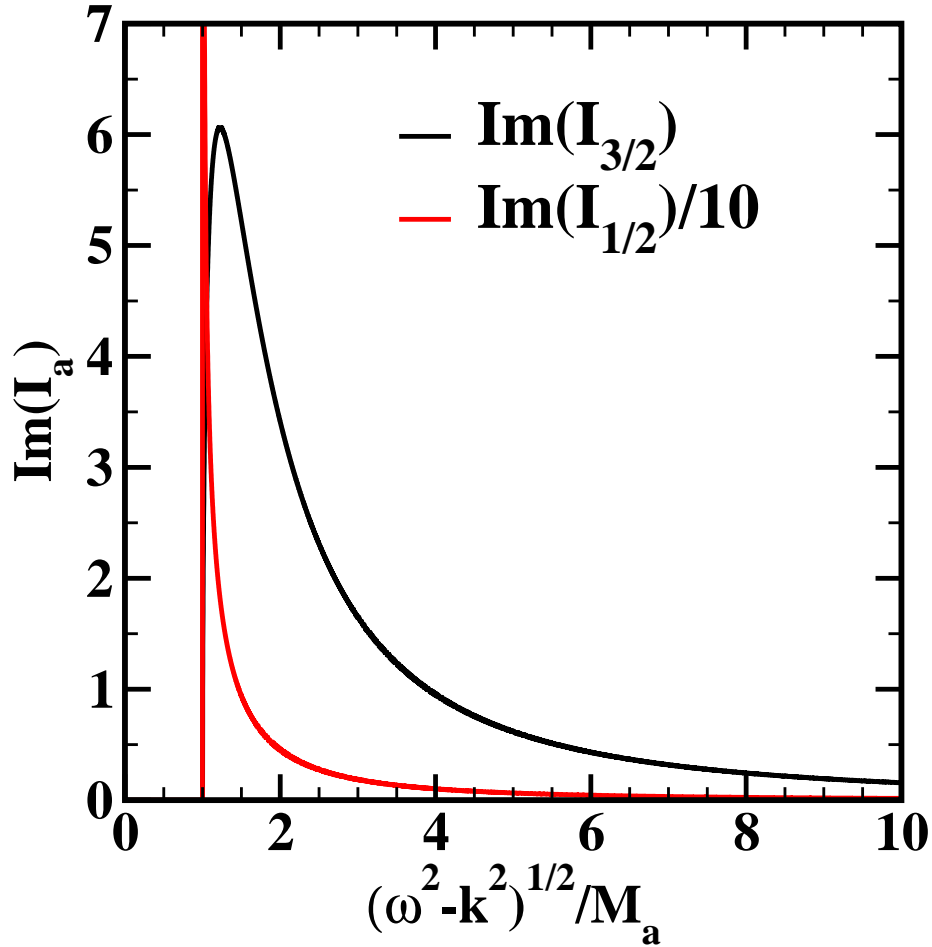


FIG. C.1: The spectral weight of the baryon Green's functions plotted vs  $\sqrt{(\omega^2 - k^2)}/M_a$  of the nucleons and  $\Delta$ -baryons.

- [7] A. O. Gogolin, A. A. Nersisyan, and A. M. Tsvelik, *Bosonization and Strongly Correlated Systems* (Cambridge University Press, Cambridge, England, 1998).
- [8] P. Di Francesco, P. Mathieu, and D. Sénéchal, *Conformal Field Theory* (Springer, Berlin, 1997).
- [9] V. P. Yurov and A. B. Zamolodchikov, *Int. J. Mod. Phys. A* **5**, 3221 (1990); **6**, 4557 (1991).
- [10] R. M. Konik and Y. Adamov, *Phys. Rev. Lett.* **98**, 147205 (2007); **102**, 097203 (2009).
- [11] R. M. Konik, T. Pálmai, G. Takács, and A. M. Tsvelik, *Nucl. Phys. B* **899**, 547 (2015).
- [12] D. Gepner, *Nucl. Phys. B* **252**, 481 (1984).
- [13] I. Affleck, *Nucl. Phys. B* **265**, 448 (1986).
- [14] G. t'Hooft, *Phys. Rep.* **142**, 357 (1986).

- [15] M. Alford, K. Rajagopal, and F. Wilczek, Phys. Lett. B **422**, 247 (1998); R. Rapp, T. Schäfer, E. V. Shuryak, and M. Velkovsky, Phys. Rev. Lett. **81**, 53 (1998).
- [16] P. Lecheminant, E. Boulat, and P. Azaria, Phys. Rev. Lett. **95**, 240402 (2005); S. Capponi, G. Roux, P. Lecheminant, P. Azaria, E. Boulat, and S. R. White, Phys. Rev. A **77**, 013624 (2008).
- [17] see, for example, in A. M. Tsvetlik *Quantum Field Theory in Condensed Matter Physics*, (Cambridge University Press, Cambridge, England, 2000).
- [18] V. G. Knizhnik and A. B. Zamolodchikov, Nucl. Phys. B **247**, 83 (1984).
- [19] I. Affleck, Nucl. Phys. B **265**, 409 (1986).
- [20] A. M. Tsvetlik, Sov. Phys. JETP **66**, 754 (1987).
- [21] G. Delfino and G. Mussardo, Nucl. Phys. B **516**, 675 (1998).
- [22] M. Fabrizio, A. O. Gogolin, and A. A. Nersisyan, Phys. Rev. Lett. **83**, 2014 (1999); Nucl. Phys. B **580**, 647 (2000).
- [23] A. Kitaev, Ann. of Phys. **321**, 2 (2006).
- [24] M. Kormos, Nucl.Phys. **B744**, 358 (2006).
- [25] Z. Bajnok, L. Palla, G. Takács, and F. Wágner, Nucl. Phys. B **601**, 503 (2001).
- [26] M. Lencsés and G. Takács, JHEP **1509**, 146 (2015).
- [27] P. Giokas and G. Watts, arXiv:1106.2448 [hep-th].
- [28] M. Hogervorst, S. Rychkov and B. C. van Rees, Phys. Rev. D **91** (2015) 025005 [arXiv:1409.1581 [hep-th]].
- [29] S. Rychkov and L. G. Vitale, Phys. Rev. D **91**, 085011 (2015) [arXiv:1412.3460 [hep-th]].
- [30] M. Lüscher, Comm. Math. Phys. **104**, 177 (1986); T. R. Klassen and E. Melzer, Nucl. Phys. B **362**, 329 (1991).
- [31] I. Affleck and F. D. M. Haldane, Phys. Rev. B **36**, 5291 (1987).
- [32] A. B. Zamolodchikov and V. A. Fateev, Sov. Phys. JETP **62**, 215 (1985).
- [33] N. Reshetikhin and F. A. Smirnov, Comm. Math. Phys. **131**, 157 (1990).
- [34] E. Witten, Nucl. Phys. B **223**, 422 (1983); E. Witten, Nucl. Phys. B **223**, 433 (1983).
- [35] A.B. Zamolodchikov and V.A. Fateev, Sov. J. Nucl. Phys. **43**, 657 (1986).